



A method for determining surface tension, viscosity, and elasticity of gels via ultrasonic levitation of gel drops

X. Shao, 1 S. A. Fredericks, 2 J. R. Saylor, 1,a) and J. B. Bostwick 1

ABSTRACT:

A method for obtaining the elasticity, surface tension, and viscosity of ultrasonically levitated gel drops is presented. The drops examined were made of agarose, a hydrogel. In contrast to previous studies where fluid properties are obtained using ultrasonic levitation of a liquid drop, herein the material studied was a gel which has a significant elasticity. The work presented herein is significant in that gels are of growing importance in biomedical applications and exhibit behaviors partially determined by their elasticities and surface tensions. Obtaining surface tension for these substances is important but challenging since measuring this quantity using the standard Wilhelmy plate or DuNuoy ring methods is not possible due to breakage of the gel. The experiments were conducted on agarose gels having elasticities ranging from 12.2 to 200.3 Pa. A method is described for obtaining elasticity, surface tension, and viscosity, and the method is experimentally demonstrated for surface tension and viscosity. For the range of elasticities explored, the measured surface tension ranged from 0.1 to 0.3 N/m, and the viscosity ranged from 0.0084 to 0.0204 Pa s. The measurements of surface tension are, to the authors' knowledge, the first obtained of a gel using ultrasonic levitation. © 2020 Acoustical Society of America. https://doi.org/10.1121/10.0001068

(Received 25 July 2019; revised 13 March 2020; accepted 23 March 2020; published online 22 April 2020)

[Editor: Veerle Keppens] Pages: 2488–2498

I. INTRODUCTION

Ultrasonic levitation of drops and bubbles has been used for some time as a method for measuring fluid properties. ^{1–12} The overall approach typically relies on the development of an ultrasonic standing wave field which is amplitude modulated to cause quadrupole shape mode oscillations of the drop. Characteristics of the drop's oscillation are then used to extract one or more fluid properties. The analytical development for how the acoustic radiation pressure interacts with the drop to determine drop shape and oscillation characteristics has been explored by several researchers. ^{3,13–15}

Much work has been done on the use of ultrasonic levitation to measure interfacial tension. Marston³ presented a theoretical development showing how the quadrupole response of a drop or bubble could be used to measure the interfacial tension, and this approach was experimentally demonstrated by Marston and Apfel² for a benzene drop in water, showing that the quadrupole oscillatory characteristics were in agreement with tabulated values of interfacial tension for benzene. Marston and Apfel⁴ investigated a drop of p-xylene in water, obtaining a value of interfacial tension that deviated from that obtained using a DuNuoy ring tensiometer measurement by only 4%. This approach was further explored by Hsu and Apfel⁵ who also developed an approach to account for finite viscosity effects and conducted preliminary measurements of changes in interfacial tension with increasing surfactant concentration on the drop

Surface tension and viscosity can be obtained by ultrasonically levitating drops, where the general approach is to use characteristics of the drop oscillation frequency and dissipation to extract both fluid properties. This can be achieved via a transient approach wherein a drop is excited into prolate-oblate shape oscillations, the excitation source is eliminated, and then the decay in drop oscillation is measured. The frequency and damping constant of the decaying signal are then used to obtain surface tension and viscosity. This approach was reviewed and used in a recent publication by Kremer et al. 10 and was shown by Holt et al. 12 to be effective in measuring the difference in the viscosity of normal blood and the blood of individuals with sickle cell disease. A more common approach for obtaining viscosity and surface tension is to obtain the steady-state frequency response function of a drop. In this method, a modification of which is the subject of the present work, the amplitude

¹Department of Mechanical Engineering, Clemson University, Clemson, South Carolina 29634, USA

²Department of Mechanical Engineering, University of Minnesota, Minneapolis, Minnesota 55455, USA

surface. Further studies on surfactant measurements were conducted by Tian *et al.*^{8,9} who measured both the surface elasticity (not to be confused with the bulk elasticity examined herein) and surface dilational viscosity of surfactants on levitated drops. Trinh and Hsu⁶ suggested the possibility of obtaining the surface tension of an ultrasonically levitated drop by measuring the outline of the equilibrium shape of the drop and extracting surface tension using the equation for the drop shape obtained from a balance of the relevant forces (see also Marston³ and Marston *et al.*¹³). Trinh *et al.*⁷ used amplitude modulation of ultrasonically levitated drops to measure the surface tension of water, hexadecane, silicone oil, and water-glycerin mixtures.

a) Electronic mail: jsaylor@clemson.edu

modulation frequency is scanned through a range near the natural frequency of the drop and the response of the drop is recorded. By treating the drop as a forced damped oscillator, its response can be described as (following the treatment of Hosseinzadeh and Holt¹¹)

$$\frac{x}{A} = \frac{1}{\sqrt{\left(1 - \left(\frac{\omega}{\omega_n}\right)^2\right)^2 + \left(2\zeta\left(\frac{\omega}{\omega_n}\right)\right)^2}},\tag{1}$$

where A is the driving amplitude, ω and ω_n are the driving frequency and natural frequency, respectively, ζ is the damping coefficient, and x is the amplitude of drop oscillation. Obtaining ω_n and ζ from experimentally obtained $(x/A, \omega)$, values for viscosity μ and surface tension σ can then be obtained from Lamb's¹⁶ equations for the n=2 quadrupole shape mode of spherical oscillation for a drop of radius R and density ρ ,

$$\omega_n^2 = \frac{8\sigma}{\rho R^3} \tag{2}$$

and

$$\zeta = \frac{5\mu}{\rho R^2 \omega_n}.\tag{3}$$

This approach has been used by Trinh and co-workers, 17,18 Hosseinzadeh and Holt, 11 and others. In the above, it should be noted that Eq. (1) is a simplified version of the more general case presented by Marston³ and Marston and Apfel,⁴ where terms for viscous dissipation in the boundary layer near the interface as well as viscous dissipation in the flow far from the interface are included [the terms that include " α " in Eqs. (6) and (7) of Marston and Apfel⁴]. For the conditions here where the drops are on the order of a millimeter, the gel and air densities are on the order of 1000 and 1 kg/m³, respectively, and the absolute viscosities of gel and air are on the order of 10^{-3} and 10^{-6} Pa s, respectively, the general result of Marston³ and Apfel and Marston⁴ reduces to Eq. (1). Similarly, Eq. (3) is a simplified equation for the case where viscous dissipation due to boundary layer effects is neglected [again eliminating α terms in Eqs. (6) and (7) of Marston and Apfel⁴ and noted in other works ^{19–21}].

In all of the above investigations, the drops which were studied were liquids and lacked elasticity. The motivation of the present work is to develop a method for obtaining the fluid properties of a drop composed of a hydrogel which has significant surface tension, viscosity, and elastic modulus. We are unaware of attempts to do this using ultrasonically levitated drops. It is noted that McDaniel and Holt²² obtained the elasticity of aqueous foam drops via the acoustic levitation approach. Viscous dissipation and surface tension were not considered in that work. Below, we develop an approach for obtaining the frequency response of ultrasonically levitated gel drops and using this information to extract the surface tension, viscosity, and elasticity of that

gel drop. This approach is then experimentally demonstrated for obtaining surface tension and viscosity, with the experimental demonstration of obtaining elasticity left as future work.

The present work focuses on gels, specifically hydrogels. These materials, often referred to as soft solids, are unique in that both surface tension and elasticity can be roughly comparable in magnitude. Drops composed of a gel material, therefore, differ from the studies discussed above which concern liquids for which surface tension is the only restoring force during drop oscillation. That soft solids have surface tension and the importance of surface tension in these materials is illustrated by the rapidly growing field of elastocapillarity in which both elasticity and capillarity affect the physics. $^{23-25}$ Surface tension σ becomes important when the characteristic length L of the system is of the same size as the elastocapillary length $\ell_e \equiv \sigma/G$, where G is the shear modulus of the gel. When $L < \ell_e$, the gel is subject to capillarity as observed in recent experiments; e.g., gravitydriven²⁶ and capillary breakup of a solid cylinder²⁷ and planar elastocapillary waves.^{28,29} Surprisingly, recent work by Style *et al.*³⁰ has shown that for soft elastomers ($G \sim 1 \text{ kPa}$) the elastic strength actually increases with liquid inclusion concentration, in direct contrast to classic Eshelby theory of inclusions, ³¹ and the magnitude of the increasing stiffness is directly proportional to the surface tension of the elastomer. The aforementioned applications highlight the critical need to be able to measure the surface tension of soft gels. The measurement technique described herein enables determination of surface tension for these elastomer composites which will allow one to optimize/design such composite materials with minimal inclusions for a desired strength. This is especially important given that the standard DuNuoy ring and Wilhelmy plate measurement methods^{32,33} are not possible for gels, since the measurement itself would break the gel. We note in passing that the surface tension of liquids can be measured using the pendant drop method, wherein the image of the drop outline is used in combination with the Young-Laplace equation to obtain the surface tension value. 34,35 While application of this approach to gels would not suffer the physical problems associated with Wilhelmy plate or Du Nuoy ring measurements, we are not aware of any theory that would enable extraction of the elasticity and surface tension using this approach.

Gels have grown in importance in recent years due to their use in various bio-printing technologies such as cell printing and tissue engineering which employs the basic principles of inkjet printing but adapted to bioinks. 36,37 Bioinks are typically hydrogels that are capable of sustaining biological function. They have complex rheologies characterized by surface tensions and elasticities that are both significant. Typically, a cell/gel mixture is forced through a nozzle, creating a drop containing (usually) a single cell which then impacts a substrate. Repetition of this process can be used to build up engineered tissues. Cell viability in such processes is linked to the strains experienced by the cell within the gel drop during the printing process. 38 These

strains are in turn partially determined by the surface tension and elasticity of the gel drop. Hence, development of bioprinting technologies requires an ability to know (*viz.*, an ability to measure) the surface tension of gels.

Herein we extend to gel drops the method of obtaining fluid properties of liquid drops and foams via ultrasonic levitation. While viscosity, elasticity, and surface tension are all important, only surface tension and viscosity are experimentally obtained by the method presented herein, and elasticity is measured independently via a standard method.

As will be shown later in this paper, the reason we were unable to measure elasticity using the method presented here is due to the moderate amount of noise in the system. This, coupled with a relatively small range in *R* in the drops studied, precluded obtaining elasticity experimentally. We note that the theory developed herein enables obtaining measurements of elasticity in principle.

Details surrounding this point are further discussed in Sec. IV.

II. EXPERIMENTAL METHOD

A. Droplet levitation and modulating the acoustic force

The experimental setup is illustrated in Fig. 1. As indicated, an ultrasonic transducer is used to levitate the gel drop. A camera and light emitting diode illumination source was used to image the gel drop and obtain its size, with the illumination source backlighting the drop. The transducer consists of a horn and reflector, following the general procedure of Trinh.³⁹ The horn and reflector are separated by an integer number of half wavelengths, with the drop levitated at one of the nodes. Two pre-stressed PZT transducers (Channel Industries, Inc.) were used in the horn, and each had an outer diameter of 46 mm, an inner diameter of 16 mm and a thickness of 3.2 mm. The transducer was driven by an Agilent 33220 A function generator, Kron-Hite amplifier (7500) combination. A carrier wave was created by the function generator at the nominal resonant frequency of the transducer which was 30.3 kHz. The actual resonance frequency varied due to variances in manufacturing tolerances, the degree of coupling between the PZT and the transducer components due to the clamping force holding the PZT in place, as well as temperature variations due to self-heating. The carrier wave was amplitude modulated at a range of frequencies near the resonant frequency of the drop, which was on the order of 100 Hz, two orders of magnitude lower in frequency than the carrier wave. During an experiment, the AM frequency was swept from below to above the drop resonant frequency. A code written in LABVIEW was used to control the drop levitation and AM frequency sweep. The AM frequency sweep typically took 3 min.

The transducer was initially tuned by adjusting the distance between the reflector and horn to most effectively levitate a drop. Then, the carrier wave frequency was adjusted to do the same. The process was iterated to achieve maximum levitation. From this point forward, resonance of the transducer could drift due to heating of the transducer and changes in temperature and humidity of the air. This drift would rarely exceed 10 Hz, but this was large enough to prevent effective levitation of drops. To address this, a software control in LABVIEW was used to adjust the carrier wave frequency between AM frequency sweeps to maintain transducer resonance as shown in Fig. 2. The applied voltage and current to the transducer were measured with a Measurements Computing data acquisition module (USB-2020 DAC) at a sample rate of 10 MHz. The phase shift between these two signals was calculated, and the carrier wave frequency was adjusted to keep the phase shift as close as possible to zero, which maximizes the power applied to the ultrasonic levitation system. The carrier wave frequency was adjusted 3 times per second. The overall method for drop levitation is similar to that presented in Fredericks and Saylor.⁴⁰

The amplitude of gel drop oscillation was measured using a laser light extinction approach similar to that of Marston, 41 as shown in Fig. 1. A helium-neon laser beam (632.8 nm wavelength) was expanded to \sim 5 mm and directed at the levitated gel droplet. The resulting occluded beam strikes an optical detector whose output is a linear function of the light intensity striking the detector. By

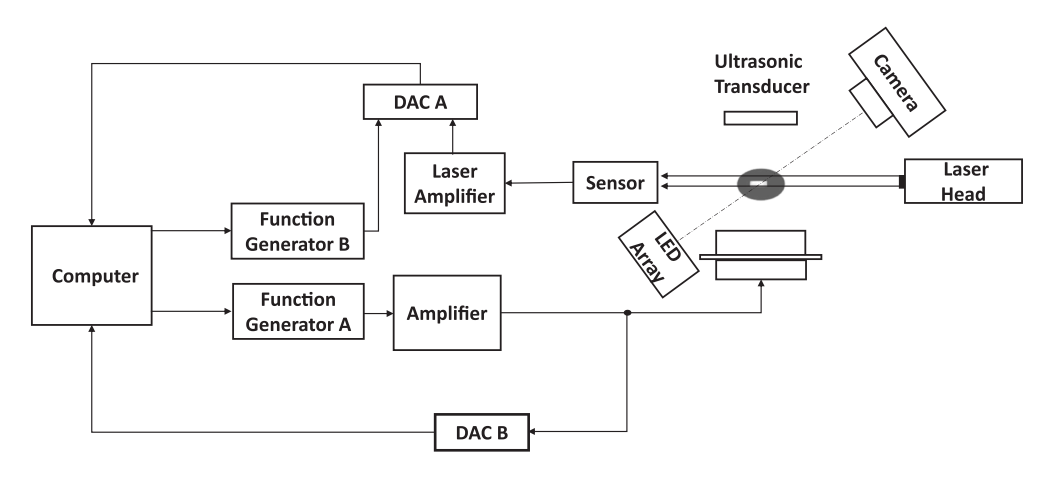


FIG. 1. Schematic of the experimental apparatus.

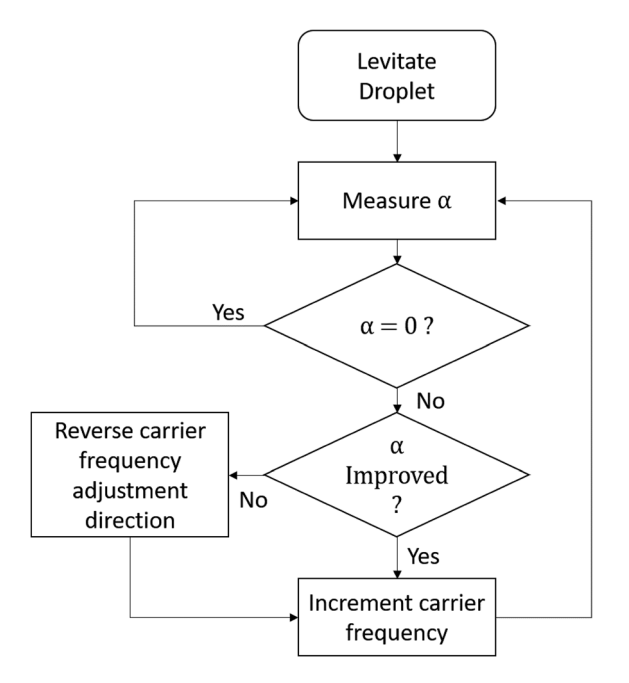


FIG. 2. Flow chart depicting the method for adjusting the carrier wave frequency by monitoring the phase shift α .

placing a plate with a 3 mm diameter hole in front of the detector, the output is proportional to the fraction of the laser light that is occluded by the oscillating drop. Hence, the output voltage of the photodetector is linearly related to the projected area of the levitated droplet, which is taken as the amplitude of oscillation. It is noted that for small oscillation amplitudes, this voltage is proportional to the change in drop radius. The frequency of the detector signal is equal to the oscillation frequency of the levitated drop. For each frequency in the AM scan, 5s of data were acquired. Then the frequency was increased and another 5 s of data were obtained. The frequency was increased in increments of 1 Hz, and a scan consisted of 30 frequencies. The amplitude of the resulting drop oscillation at each excitation frequency was obtained by taking the FFT of the last 4 s of each 5 s time trace. The first second of each trace was discarded to remove any influence of the previous AM frequency. The amplitude obtained from this FFT is referred to as x and the amplitude of the driving frequency is referred to as A in Eqs. (1) and (4) presented below. Each experiment resulted in a point in the plot of the amplitude of drop oscillation versus excitation frequency. The natural frequency was taken to be the frequency at which a maximum in the drop oscillation was observed.

B. Formation of gel drops

Following the approach of Tokita and Hikichi, ⁴² hydrogels were prepared by dissolving agarose powder (Sigma Aldrich type VI-A) in doubly distilled water (though Tokita and Hikichi used de-ionized water) at 90 °C for 1 h. Our goal was to create gelled drops that were as close to spherical as possible. We initially allowed the drop to gel on a Teflon surface, and also experimented with letting the drop

gel while ultrasonically levitated. However, both of these approaches resulted in relatively oblate drop shapes along with significant changes in the drop size due to evaporation. Herein we followed the method of Chakrabarti⁴³ and created a liquid mixture having a density gradient spanning the density of the gel. Specifically, we partially filled a beaker with silicone oil (PDM-7040, Gelest) having a density of $\rho = 1.07$ g/ml, and above this we poured *n*-octane (Acros Organics), having a density of $\rho = 0.7$ g/ml. Both silicone oil and n-octane are not miscible in agarose. The agarose solutions we used had a nominal density of $\rho = 1.0$ g/ml, and when placed in the beaker the agarose drops quickly migrated to the interface of the two liquids and exhibited a highly spherical shape as shown in the image of a sample gel drop presented in Fig. 3. Figure 4 shows one of these drops levitated in the ultrasonic standing wave field without amplitude modulation, showing that the equilibrium shape, though not as spherical as in Fig. 3, is still quite round. In addition to generating spherical drops, this approach also had the benefit of allowing gelation without evaporation, ensuring that the agarose/water concentration did not change during gelation. After allowing these drops to gel at room temperature for at least 3 h, a drop was removed from the silicone oil/n-octane beaker after which it was carefully washed in *n*-heptane (Fisher Chemicals) for 2 min to remove any excess silicone oil or octane. The drop was then washed

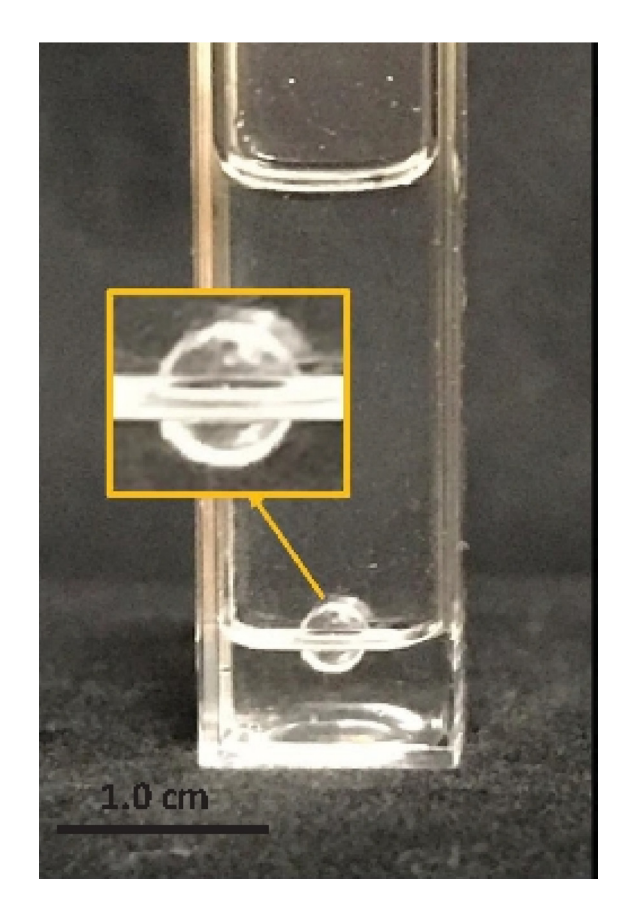


FIG. 3. (Color online) Image of a gel drop located at the interface between silicone oil and n-octane in a cuvette. The gel drop has a diameter of 2.86 mm and the gel has an elasticity of $G = 13.0 \, \text{Pa}$.

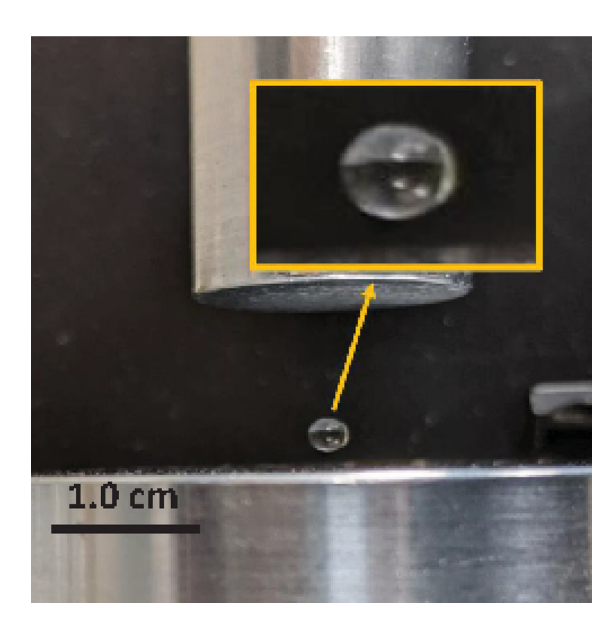


FIG. 4. (Color online) Image of a gel drop levitated in an ultrasonic standing wave field. The amplitude modulation is zero in this case, showing the equilibrium shape of the drop in the field. The gel drop diameter is $2.82 \, \mathrm{mm}$ and the elasticity is $G = 13.0 \, \mathrm{Pa}$.

once more with a fresh solution of n-heptane. After this, the drop was inserted into the levitation system and an experiment was initiated after allowing 15 s to pass so that any remaining heptane evaporated. Multiple drops were made from the same agarose solution ensuring that the concentration and hence the elasticity were the same when doing multiple runs. Drops made in this way were kept in the silicone oil/n-octane beaker until needed. For the work presented here, the drop radius varied from R = 1.16-1.6 mm, and the agarose concentration varied from 0.106 to 0.285 wt. %.

For each concentration of agarose gel used in these experiments, the complex modulus G = G' + iG'' for that gel was obtained using an Anton Paar rheometer (MCR 302). This method employs a small Petri dish in which the gel solution is placed and allowed to gel. The rheometer then contacts the surface of the gel with a disk. Dynamic oscillatory shear tests over a range of frequencies from 1 to 50 rad/s were then obtained. Prior to these measurements, a small amount of silicone oil was placed over the annular region between the disk and the edge of the Petri dish, preventing evaporation during the course of the measurement. For the gels used here, the loss modulus G'' was found to be over one order of magnitude smaller than the storage modulus G' and G'' is ignored hereinafter. This behavior has been demonstrated for agarose by other authors as well, for example, Monroy and Langevin²⁸ who showed that the loss modulus was at least one order of magnitude smaller than the storage modulus for 0.2 wt. % agarose hydrogels (very similar to the 0.106-0.285 wt. % agarose hydrogels explored here) over a frequency range from 10^{-2} to 10^2 Hz. Thus, the agarose hydrogels used in our experiments behave as linear elastic solids. For simplicity, the storage modulus G' is referred to as G hereinafter. For the gels investigated here, G ranged from 12.2 to 200.3 Pa over the agarose concentrations explored. The 95% confidence interval for measurement of G was 5.6 Pa which included the instrument uncertainty and experimental uncertainty obtained from measuring several samples of the same gel. For each value of G explored, at least three experimental runs were conducted, except for the case when G = 38 Pa when two runs were conducted. An average of 3.6 experiments were run for each value of G.

III. RESULTS

A. Theoretical model

Obtaining surface tension, elastic modulus, and viscosity, σ , G, and μ , from the results presented above requires a model relating the driving frequency and drop oscillation amplitude to the natural frequency and damping coefficient as was done for just σ and μ using Eqs. (1)–(3) in Sec. I. This is done by developing an equation for the oscillations of a sphere having non-zero elasticity, viscosity, and surface tension.

Here we begin by following the general approach presented in Hosseinzadeh and Holt, which is a simplification of that presented by Marston³ for the case of negligible boundary layer dissipation and which exploits the similarity of the oscillating drop with the damped-driven oscillator, an approach which has been exploited in the study of drops and bubbles in different ways by a range of researchers, 16,44–52

$$\ddot{x} + 2\zeta \omega_n \dot{x} + \omega_n^2 x = A\cos\omega t,\tag{4}$$

where ζ is the damping ratio, ω_n the natural frequency, and (A,ω) the driving amplitude and frequency, respectively. In the harmonic oscillator structure, inertia acts as the "mass," the resistive force of surface tension and elasticity as the "spring constant," and viscous dissipation as the "damping constant," all of which are determined by projecting onto a particular interface shape $\eta(\theta,\varphi,t)$. Our drop oscillates in the fundamental mode $\eta(\theta,\varphi,t)=x(t)P_2(\cos\theta)$, where P_2 is the Legendre polynomial of order n=2, 53 and we project onto this mode, which is axisymmetric and oscillates between an oblate and prolate shape.

Each component of the essential physics that enters into our model is schematically viewed as a spring or dashpot whose constant is normalized with respect to the drop mass. These relationships have been individually determined in the literature. ^{16,54,55} Damping is associated with viscous dissipation of a fluid which was computed by Lamb using the potential flow solution for the spherical drop ¹⁶ and assuming negligible viscous dissipation due to boundary layer effects; this gives ζ in Eq. (3). Both surface tension and elasticity resist deformation like a spring and we idealize these two forces as springs acting in parallel so that we can superimpose their effects. We note that this, along with an assumption of a constant value for (σ, μ, G) , independent of drop deformation, restricts us to Newtonian materials whose elasticity and surface tension do not interact. The spring

constant due to surface tension is given by Eq. (2) assuming an inviscid liquid drop.⁵⁴ The spring constant due to elasticity is computed from a nonlinear characteristic equation which is derived in the Appendix to give

$$\eta(\eta^2 - 10)j_2(\eta) - 2(\eta^2 - 16)j_3(\eta) = 0$$
 (5)

for the scaled elastic frequency

$$\eta = \omega R \sqrt{\rho/G} \tag{6}$$

with j_l the spherical Bessel function, assuming an incompressible spherical globe, ⁵⁵ which admits a numerical solution $\eta = 2.665$ that when rearranged gives the spring constant due to elasticity

$$\omega_n^2 = (2.665)^2 \frac{G}{\rho R^2}. (7)$$

There is no explicit coupling between surface tension and elasticity in the above development, and to our knowledge no such model exists for a spherical drop. Combining the spring constants due to surface tension and elasticity gives an effective spring constant

$$\omega_n^2 = \frac{1}{\rho R^3} \left[8\sigma + (2.665)^2 GR \right],\tag{8}$$

which can be combined with the damping ratio ζ in Eq. (3) in the system response, Eq. (1). This enables a relationship between driving frequency and drop oscillation amplitude to (σ, μ, G) . Specifically, using the $(x/A, \omega)$ data from any given gel drop levitation run and fitting it to Eq. (1) using ω_n and ζ as fitting parameters, the resulting (ω_n, ζ) can be obtained and used to get μ from Eq. (3), and G and σ from Eq. (8) by doing multiple runs with gel drops having different R.

B. Experimental results

While experiments were indeed conducted at different R for gels of the same concentration, the range in R was small and increasing this range was challenging due to difficulties in forming small drops and in stably levitating large drops. This, combined with scatter in the data, made difficult the extraction of (σ, μ, G) from the experiments using the approach outlined above. Instead, G was measured as described in Sec. II, and is used as an input while (σ, μ) are extracted from the experimentally obtained (ω_n, ζ) .

Figure 5 is a plot of drop oscillation amplitude scaled to the driving amplitude versus driving frequency for a sample run where the elasticity of the gel was 32 Pa. Along with this plot are images of a gel drop undergoing shape mode oscillations over the entire period of the oscillation. The solid line in the plot was obtained by fitting the data using Eq. (1). As noted in Sec. II the frequency at which the peak in this plot is observed is taken as the natural frequency. In Fig. 5, the peak is located at a frequency of 99.32 Hz, and was identified using the fit to the data as opposed to the data alone, since the fit incorporated information from multiple data points and was therefore less sensitive to a spurious measurement. It is also noted that while measurements were obtained at 30 excitation frequencies for each drop, only 21 were used (and presented in Fig. 5) because data points obtained far from resonance exhibited greater scatter.

The results of all the runs are presented in Figs. 6 and 7 showing how the natural frequency of the gel drop varies with G. In Fig. 6, the natural frequency is scaled to the capillary natural frequency given in Eq. (2) (designated ω_{σ} in the figure), and in Fig. 7 the natural frequency is scaled to the elastic frequency, Eq. (7) (designated ω_{G} in the figure). In both of these plots and those to follow, the vertical error bars are the 95% confidence intervals for that value of G. As noted in Sec. II, the 95% confidence interval for G was only 5.6 Pa, and horizontal error bars are not included since this

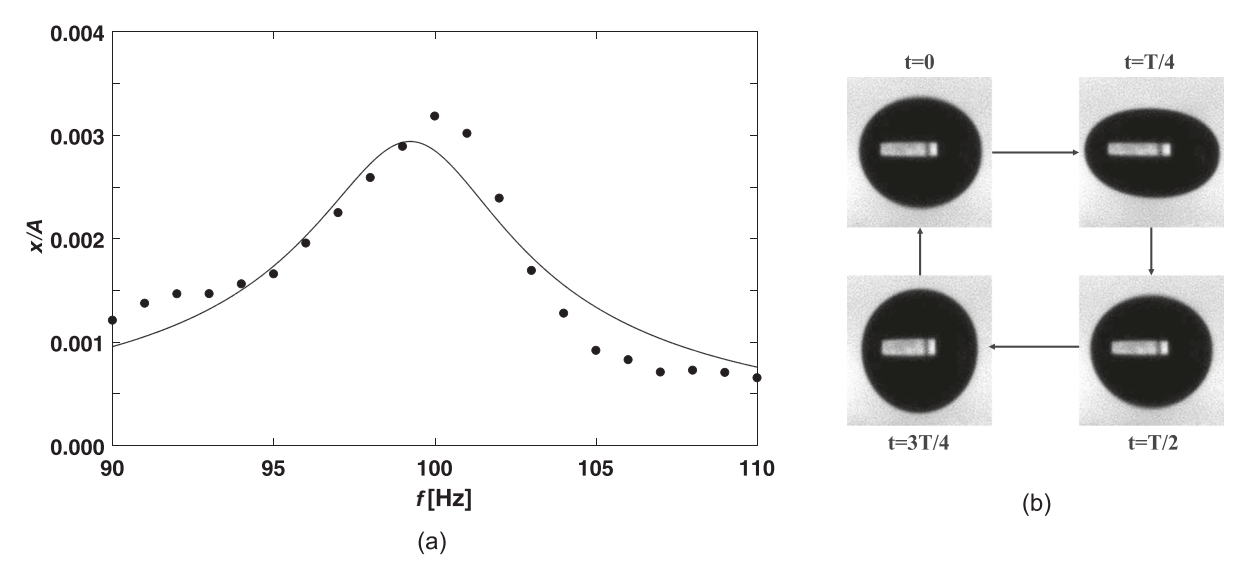


FIG. 5. (a) Plot of oscillation amplitude versus excitation frequency f for a sample run where the elasticity was G = 32 Pa. (b) Image of a gel drop undergoing a full period of shape mode oscillation. The drop radius was R = 1.43 mm in this particular experiment.

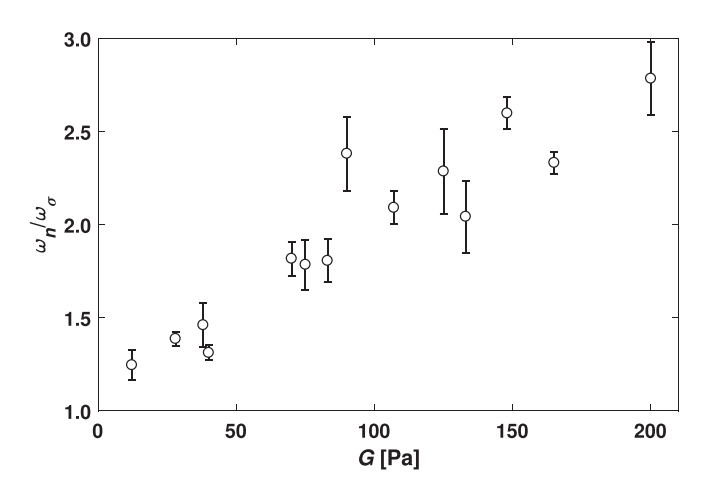


FIG. 6. Plot of the gel drop natural frequency scaled to the capillary natural frequency versus elasticity G.

magnitude in uncertainty is smaller than the width of the symbols in these figures.

The fact that in neither Fig. 6 nor Fig. 7 is the scaled frequency a constant demonstrates that both surface tension and elasticity are playing a role in the gel drop dynamics, as expected. It also shows that σ must be varying with the agarose concentration since a constant value for σ independent of that concentration (which would translate to a constant σ independent of G) should give a horizontal line in the plot of ω_n/ω_G in Fig. 7, which is not the case.

Applying the theory developed in Sec. II, each data point presented in the above plots can be translated into a viscosity and surface tension, and these are presented in Figs. 8 and 9, respectively. The linear fits presented in Figs. 8 and 9 are

$$\mu = 6.005 \times 10^{-5} G + 0.008384 \tag{9}$$

and

$$\sigma = 0.001022G + 0.07229,\tag{10}$$

respectively.

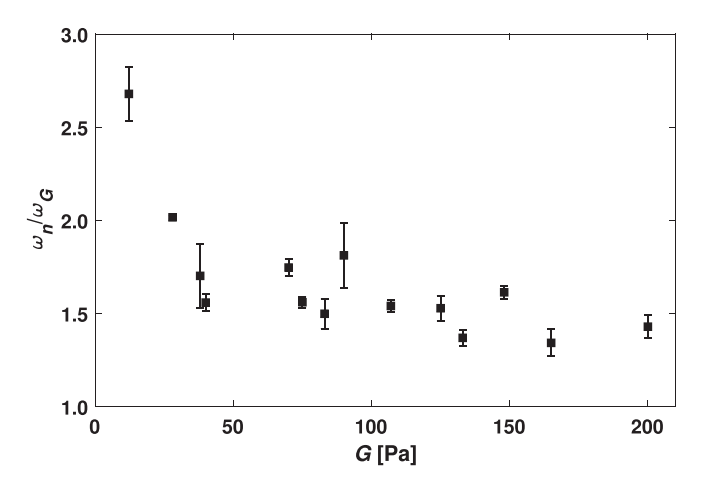


FIG. 7. Plot of the gel drop natural frequency scaled to the natural frequency of a purely elastic drop versus elasticity G.

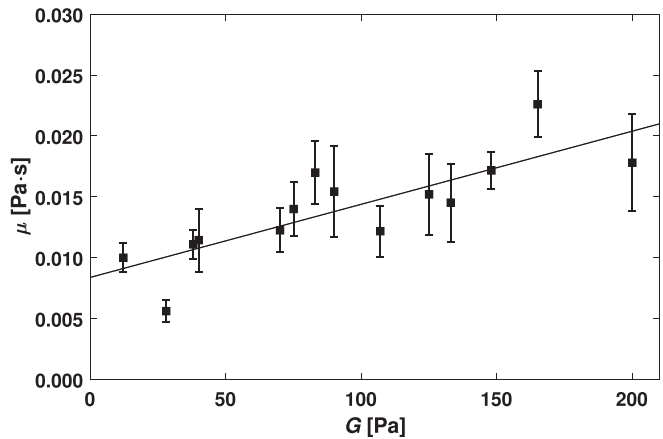


FIG. 8. Plot of viscosity μ versus elastic modulus G with linear curve fit.

It is noted that obtaining μ via the method described above is more sensitive to errors in data points that were far from the natural frequency. Hence, in obtaining μ , a total of nine data points were used, the data point at the natural frequency and four above and below that frequency. Since frequency scans were obtained in 1 Hz increments, this corresponds to a range of 8 Hz in frequency when obtaining μ . This approach resulted in less scatter in the data than when using the entire data set since data farther from the resonance point was sometimes spurious in nature, occasionally exhibiting an amplitude higher than that at the natural frequency.

IV. DISCUSSION

Figures 8 and 9 demonstrate the ability of the described method to obtain (σ,μ) for levitated gel drops. The ability to obtain σ is especially noteworthy since we are aware of no other means for obtaining surface tension for a gel. Of course, this also means that we are unable to compare our results to other data or methods. However, by setting G=0 in Eq. (10), we obtain an extrapolated value of $\sigma=0.0723$ N/m for the pure water case, which is essentially the exact value of σ for pure water at STP. ⁵⁶

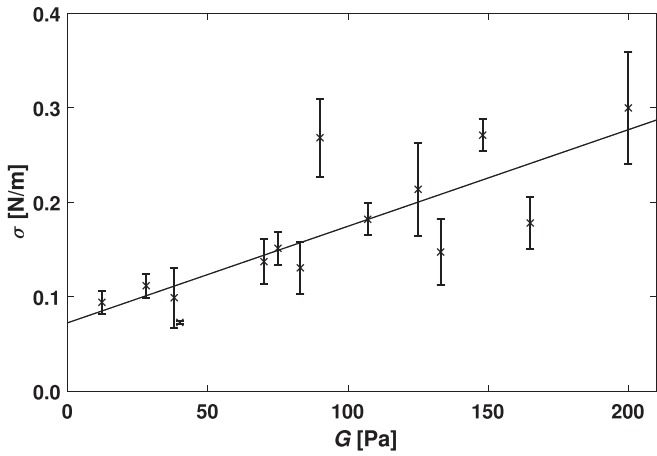


FIG. 9. Plot of surface tension σ versus elastic modulus G with linear curve fit.

We should note that the viscosity presented here is not the viscosity as it is typically understood, viz., the constant which relates the shear stress to the velocity gradient in a flowing liquid, since we are considering gels, which do not flow. Hence, μ is simply the quantity which accounts for energy dissipation in the deforming gel drop. Indeed, when we set G=0 in Eq. (9), we obtain $\mu=0.00838$ Pa s which differs from the value of pure liquid water at STP by a factor of 10, a result which is likely due to the change in what μ in Eq. (3) represents when a liquid becomes a gel and ceases to admit flow, even at very small G.

With regard to the measurement of physical properties by exciting shape oscillations in ultrasonically levitated drops, it should be noted that Hosseinzadeh and Holt¹¹ demonstrate that, for liquid drops, the measurements of σ and μ could be in significant error if the oscillation amplitudes are too large. Specifically, their work contradicts the oft-cited conclusion of Becker et al.,⁵⁷ that for oscillation amplitudes less than 10%, nonlinearities would not be significant, presumably avoiding errors in measurements of σ and μ . Indeed, Hosseinzadeh and Holt¹¹ suggest that oscillation amplitudes be kept to less than 0.5% to avoid errors in measurements of σ and μ . Herein our oscillation amplitudes were all less than 5%, which is less than that suggested by Becker et al.,57 but significantly larger than that suggested by Hosseinzadeh and Holt.¹¹ Though we recognize the validity of the work of Hosseinzadeh and Holt, 11 we think that our oscillation amplitudes are sufficiently small and justify our assumption that nonlinearities are not playing a significant role in our measurements by the following arguments. First, as noted by Hosseinzadeh and Holt, 11 the previous work that they reviewed revealed surface tension measurements that underpredicted or overpredicted known values when oscillation amplitudes were large. However, when extrapolating to zero G, our Eq. (10) gives a surface tension identical to that of water. Second, for the case of viscosity, Hosseinzadeh and Holt¹¹ note that it is the deviation of the actual velocity field from the infinitesimal amplitude shape mode oscillations predicted by Lamb, ¹⁶ which is the cause for finite amplitude contributions to errors in the measurement of viscosity of ultrasonically levitated *liquid* drops. This is unlikely to be the case for the gel drops considered here where flow does not occur. Indeed, one author contends that it is only when turbulent flow occurs that a deleterious effect on viscosity measurement occurs, 58 a situation certainly not possible here. Finally, even for the case of the glycerol-water system investigated by Hosseinzadeh and Holt¹¹ (20 wt. %), their data show that even at a high 12% amplitude oscillation they see an error in the measurement of viscosity greater than 10% only for drop diameters larger than about 1.5 mm (reading off of the data presented in their Fig. 4). Our results at oscillation amplitudes of 5% or less are for drop radii ranging from 1.16 to 1.6 mm indicating that we should only see errors approach 10% for the largest of the drops we investigated. Hence, we do not see finite amplitude effects as contributing to errors in our measurements of physical properties, though we recognize that the authors we compare to above are all working with liquid systems and so it would be useful to do a study of the upper bound of oscillation amplitude for the measurement of (σ, μ, G) , in gel systems. Perhaps the best way to do this would be to conduct experiments such as those presented above, but for a larger range of R where G could be obtained (see below) and thereby compared with standard rheometer measurements of G.

As noted in Sec. III A, only (σ, μ) are obtained herein from the experimental data. It is possible to obtain (σ, μ, G) from the data, taking advantage of small differences in R for the droplets used at each value of agarose concentration. However, the range in R for these experiments was small, and the scatter in the data presented in Figs. 8 and 9 was not insignificant. However, this does not preclude using this method for obtaining G given a data set containing a wider range in R. A likely cause of the scatter is the low frequency oscillation (on the order of a few Hz) of the drop position within the ultrasonic standing wave field. Future work should focus on stabilizing the drop position, perhaps by including a shroud around the standing wave field to help block air currents in the room, and the development of a method for making gel drops capable of a large range in R. Success in these steps would enable obtaining measurements of (σ, μ, G) via this method.

V. CONCLUSIONS

A relationship was developed relating the surface tension, viscosity, and elasticity of a gel to the oscillatory characteristics of a gel drop. Experiments were conducted showing that this relationship could be applied to an ultrasonically levitated gel drop excited into shape mode oscillations to measure the surface tension and viscosity of that gel drop. Specifically, agarose gel drops were investigated having a range of elasticity from 12.2 to 200.3 Pa and the measured surface tension ranged from 0.1 to 0.3 N/m, and the measured viscosity ranged from 0.01 to 0.02 Pa s. Obtaining surface tension in this way is especially important given that existing methods for measuring surface tension (e.g., the DuNuoy ring method or Wilhelmy plate method) cannot be used for gels since they would break the gel in the process of measurement. This work extends that of previous researchers who have used ultrasonic levitation of liquids to obtain properties such as surface tension and viscosity. By extending the work of these researchers to materials having elasticity, this approach enables measurements of gel properties, an important step due to the significance of gels in cell printing and tissue engineering which employs the basic principles of inkjet printing adapted to bioinks. To our knowledge, these are the first measurements of surface tension obtained for a hydrogel using ultrasonic levitation.

ACKNOWLEDGMENTS

The authors acknowledge support from Clemson University. J.B.B. acknowledges support from NSF Grant No. CBET-1750208.

APPENDIX: DERIVATION OF CHARACTERISTIC EQUATION (5)

Consider a solid sphere of radius R whose surface is disturbed by a small perturbation which generates a time-dependent displacement field $\mathbf{U}(\mathbf{x},t)$ within the sphere. We assume a normal mode ansatz $\mathbf{U}(\mathbf{x},t) = \mathbf{u}(\mathbf{x})\mathrm{e}^{i\omega t}$ with frequency ω , and define the displacement field \mathbf{u} in a spherical coordinate system,

$$\mathbf{u}(\mathbf{x}) = u_r(r, \theta, \varphi)\hat{e}_r + u_{\theta}(r, \theta, \varphi)\hat{e}_{\theta} + u_{\varphi}(r, \theta, \varphi)\hat{e}_{\varphi},$$
(A1)

where θ and φ refer to the polar and azimuthal angles, respectively.

For a linearly elastic solid with Lame' parameters λ and G, the displacement field \mathbf{u} is governed by the Navier elastodynamic equation

$$(\lambda + G)\nabla(\nabla \cdot \mathbf{u}) + G\nabla^2 \mathbf{u} = -\rho\omega^2 \mathbf{u}, \tag{A2}$$

where ρ is the density. The stress-strain relation is given by

$$\tau = 2G + \lambda \operatorname{Tr}(\varepsilon),\tag{A3}$$

where Tr is the trace of the strain field

$$\varepsilon = \frac{1}{2} (\nabla \mathbf{u} + \nabla \mathbf{u}^T). \tag{A4}$$

The governing equation (A2) is simplified by applying the Helmholtz decomposition theorem and writing the displacement field in terms of the potential functions (ϕ, T, S) ,

$$\mathbf{u} = \nabla \phi + \nabla \times (T\hat{e}_r) + \nabla \times (S\hat{e}_r). \tag{A5}$$

Substituting Eq. (A5) into Eq. (A2) results in a set of decoupled Helmholtz equations,

$$\nabla^2 \phi + a^2 \phi = 0, (A6a)$$

$$\nabla^2 \left(\frac{T}{r}\right) + \beta^2 \left(\frac{T}{r}\right) = 0, \tag{A6b}$$

$$\nabla^2 \left(\frac{S}{r} \right) + \beta^2 \left(\frac{S}{r} \right) = 0, \tag{A6c}$$

where $a = \omega \sqrt{\rho/(\lambda + 2G)}$ and $\beta = \omega \sqrt{\rho/G}$.

The general solution of Eq. (A6) can be written by expanding the potentials ϕ , T, S in a spherical harmonic $Y_l^m(\theta, \varphi)$ basis,

$$\phi = \sum_{l=0}^{\infty} \sum_{m=-l}^{l} A_{lm} j_l(ar) Y_l^m(\theta, \varphi),$$

$$T = \sum_{l=0}^{\infty} \sum_{m=-l}^{l} r B_{lm} j_l(\beta r) Y_l^m(\theta, \varphi),$$

$$S = \sum_{l=0}^{\infty} \sum_{m=-l}^{l} r C_{lm} j_l(\beta r) Y_l^m(\theta, \varphi),$$
(A7)

where j_l is the spherical Bessel functions of the first kind, l the polar wavenumber, and m the azimuthal wavenumber. Note that we suppress the spherical Bessel function of the second kind in the solution, which diverges at the origin and is nonphysical. The unknown constants A_{lm} , B_{lm} , C_{lm} are determined from the traction-free boundary conditions at the free surface r = R.

$$\tau_{rr}(R) = \tau_{r\theta}(R) = \tau_{r\varphi}(R) = 0. \tag{A8}$$

Applying Eq. (A7) to Eqs. (A3) and (A4) allows us to express the boundary conditions (A8) in terms of the unknown constants *A*, *B*, and *C*, which satisfy

$$\frac{2G}{R^2}[A_{lm}T_{11} + C_{lm}T_{13}] = 0, (A9a)$$

$$\frac{2G}{R^2}[A_{lm}T_{31} + C_{lm}T_{33}] = 0, (A9b)$$

$$\frac{2G}{R^2}B_{lm}T_{22} = 0, (A9c)$$

where

$$T_{11} = \left(l^2 - l - \frac{1}{2}\eta^2\right) j_l(\kappa\eta) + 2\kappa\eta j_{l+1}(\kappa\eta),$$

$$T_{13} = (l-1)j_l(\kappa\eta) - \kappa\eta j_{l+1}(\kappa\eta),$$

$$T_{22} = (l-1)j_l(\eta) - \eta j_{l+1}(\eta),$$

$$T_{31} = l(l+1)\left\{(l-1)j_l(\eta) - \eta j_{l+1}(\eta)\right\},$$

$$T_{33} = \left(l^2 - 1 - \frac{1}{2}\eta^2\right) j_l(\eta) + \eta j_{l+1}(\eta).$$
(A10)

The solvability condition for Eq. (A9) gives

$$T_{11}T_{33} - T_{13}T_{31} = 0, \quad T_{22} = 0,$$
 (A11)

which admits two classes of solution; spheroidal and torsional modes. The spheroidal modes satisfy the following characteristic equation:

$$-\frac{1}{2} \left(\frac{2l^2 - l - 1}{\eta^2} - \frac{1}{2} \right) j_l(\kappa \eta) j_l(\eta)$$

$$+ \left(\frac{l^3 + l^2 - 2l}{\eta^3} - \frac{1}{2\eta} \right) j_l(\kappa \eta) j_{l+1}(\eta)$$

$$+ \left(\frac{l^3 + 2l^2 - l - 2}{\eta^3} - \frac{1}{\eta} \right) \kappa j_l(\kappa \eta) j_{l+1}(\eta)$$

$$+ \frac{2 - l - l^2}{\eta^2} \kappa j_{l+1}(\kappa \eta) j_l(\kappa \eta) = 0, \tag{A12}$$

and the torsional modes satisfy

$$(l-1)j_l(\eta) - \eta j_{l+1}(\eta) = 0. (A13)$$

Here we have scaled time with respect to the elastic shear wave timescale which admits a dimensionless frequency $\eta = \omega R \sqrt{\rho/G}$ and a compressibility factor $\kappa = G/(\lambda + 2G)$,

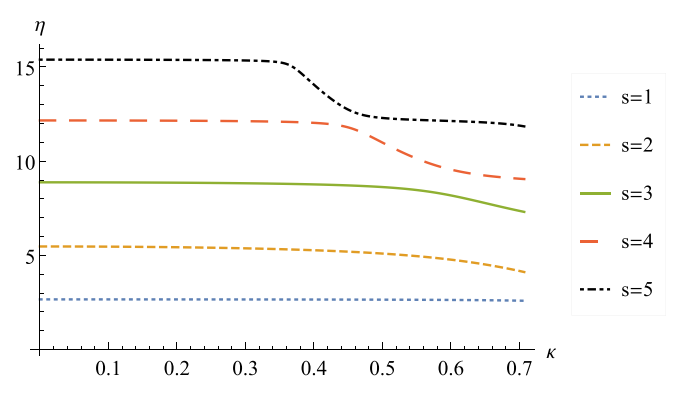


FIG. 10. (Color online) Plot of η versus κ showing the first five roots of spheroidal l=2 vibration. Here s correspond to the sth root of Eq. (A12).

which can be written with respect to the Poisson ratio ν as $\kappa = \sqrt{(1-2\nu)/2(1-\nu)}$. For an incompressible material $\nu = 1/2$ and $\kappa = 0$.

These equations have an infinite number of roots which correspond to the natural oscillation frequencies of the solid sphere. For the purposes of this paper, we are interested in the spheroidal or shape change modes and in particular the l=2 oblate-prolate mode which satisfies

$$\frac{1}{2} \left(\frac{1}{2} - \frac{5}{\eta^2} \right) j_2(\eta) j_2(\kappa \eta) + \left(\frac{8}{\eta^3} - \frac{1}{2\eta} \right) j_2(\kappa \eta) j_3(\eta)
+ \kappa \left(\frac{12}{\eta^3} - \frac{1}{\eta} \right) j_2(\eta) j_3(\kappa \eta) - \frac{4\kappa}{\eta^2} j_3(\eta) j_3(\kappa \eta) = 0.$$
(A14)

Setting $\kappa = 0$ delivers Eq. (5).

For reference, the first five roots of Eq. (A14) plotted against κ is shown in Fig. 10.

- ¹L. A. Crum, "Acoustic force on a liquid droplet in an acoustic stationary wave," J. Acoust. Soc. Am. **50**, 157–163 (1971).
- ²P. L. Marston and R. E. Apfel, "Acoustically forced shape oscillation of hydrocarbon drops levitated in water," J. Colloid Interface Sci. 68, 280–286 (1979).
- ³P. L. Marston, "Shape oscillation and static deformation of drops and bubbles driven by modulated radiation stresses—Theory," J. Acoust. Soc. Am. 67, 15–26 (1980).
- ⁴P. L. Marston and R. E. Apfel, "Quadrupole resonance of drops driven by modulated acoustic radiation pressure—Experimental properties," J. Acoust. Soc. Am. **67**, 27–37 (1980).
- ⁵C.-J. Hsu and R. E. Apfel, "A technique for measuring interfacial tension by quadrupole oscillation of drops," J. Colloid Interface Sci. **107**(2), 467–476 (1985).
- ⁶E. H. Trinh and C. J. Hsu, "Equilibrium shapes of acoustically levitated drops," J. Acoust. Soc. Am. **79**(5), 1335–1338 (1986).
- ⁷E. H. Trinh, P. L. Marston, and J. L. Robey, "Acoustic measurement of the surface tension of levitated drops," J. Colloid Interface Sci. **124**(1), 95–103 (1988).
- ⁸Y. Tian, R. G. Holt, and R. E. Apfel, "Investigation of liquid surface rheology of surfactant solutions by droplet shape oscillations: Theory," Phys. Fluids **7**(12), 2938–2949 (1995).
- ⁹Y. Tian, R. G. Holt, and R. E. Apfel, "Investigation of liquid surface rheology of surfactant solutions by droplet shape oscillations: Experiments," J. Colloid. Interf. Sci. 187, 1–10 (1997).
- ¹⁰J. Kremer, A. Kilzer, and M. Petermann, "Simultaneous measurement of surface tension and viscosity using freely decaying oscillations of acoustically levitated droplets," Rev. Sci. Instrum. 89, 015109 (2018).

- ¹¹V. A. Hosseinzadeh and R. G. Holt, "Finite amplitude effects on drop levitation for material properties measurement," J. Appl. Phys. **121**, 174502 (2017).
- ¹²V. A. Hosseinzadeh, C. Brugnara, and R. G. Holt, "Shape oscillations of single blood drops: Applications to human blood and sickle cell disease," Sci. Rep. 8, 16794 (2018).
- ¹³P. L. Marston, S. E. LoPorto-Arione, and G. L. Pullen, "Quadrupole projection of the radiation pressure on a compressible sphere," J. Acoust. Soc. Am. 69, 1499–1501 (1981).
- ¹⁴T. J. Asaki and P. L. Marston, "Equilibrium shape of an acoustically levitated bubble driven above resonance," J. Acoust. Soc. Am. 97, 2138–2143 (1995).
- ¹⁵P. L. Marston and D. B. Thiessen, "Manipulation of fluid objects with acoustic radiation pressure," Ann. N.Y. Acad. Sci. 1027, 414–434 (2004).
- ¹⁶H. Lamb, *Hydrodynamics*, 6th ed. (Cambridge University Press, Cambridge, 1932).
- ¹⁷E. Trinh and T. G. Wang, "Large-amplitude free and driven drop-shape oscillations: Experimental observations," J. Fluid Mech. 122, 315–338 (1982).
- ¹⁸E. Trinh, A. Zwern, and T. G. Wang, "An experimental study of small-amplitude drop oscillations in immiscible liquid systems," J. Fluid Mech. 115, 453–474 (1982).
- ¹⁹P. L. Marston and S. G. Goosby, "Ultrasonically stimulated low-frequency oscillation and breakup of immiscible liquid drops: Photographs," Phys. Fluids 28, 1233–1242 (1985).
- ²⁰T. J. Asaki, P. L. Marston, and E. H. Trinh, "Shape oscillations of bubbles in water driven by modulated ultrasonic radiation pressure: Observations and detection with scattered light," J. Acoust. Soc. Am. 93, 706–713 (1993).
- ²¹T. J. Asaki and P. L. Marston, "Free decay of shape oscillations of bubbles acoustically trapped in water and sea water," J. Fluid Mech. 300, 149–167 (1995).
- ²²J. G. McDaniel and R. G. Holt, "Measurement of aqueous foam rheology by acoustic levitation," Phys. Rev. E 61, R2204 (2000).
- ²³R. W. Style, A. Jagota, C.-Y. Hui, and E. R. Dufresne, "Elastocapillarity: Surface tension and the mechanics of soft solids," Ann. Rev. Condens. Matter Phys. 8, 99–118 (2017).
- ²⁴J. Bico, É. Reyssat, and B. Roman, "Elastocapillarity: When surface tension deforms elastic solids," Ann. Rev. Fluid Mech. 50, 629–659 (2018).
- ²⁵B. Andreotti and J. H. Snoeijer, "Statics and dynamics of soft wetting," Ann. Rev. Fluid Mech. **52**, 285–308 (2020).
- ²⁶S. Mora, T. Phou, J.-M. Fromental, and Y. Pomeau, "Gravity driven instability in elastic solid layers," Phys. Rev. Lett. 113(17), 178301 (2014).
- ²⁷S. Mora, C. Maurini, T. Phou, J.-M. Fromental, B. Audoly, and Y. Pomeau, "Solid drops: Large capillary deformations of immersed elastic rods," Phys. Rev. Lett. 111(11), 114301 (2013).
- ²⁸F. Monroy and D. Langevin, "Direct experimental observation of the crossover from capillary to elastic surface waves on soft gels," Phys. Rev. Lett. 81(15), 3167 (1998).
- ²⁹X. Shao, J. R. Saylor, and J. B. Bostwick, "Extracting the surface tension of soft gels from elastocapillary wave behavior," Soft Matter 14(36), 7347–7353 (2018).
- ³⁰R. W. Style, R. Boltyanskiy, B. Allen, K. E. Jensen, H. P. Foote, J. S. Wettlaufer, and E. R. Dufresne, "Stiffening solids with liquid inclusions," Nat. Phys. 11(1), 82–87 (2015).
- ³¹J. D. Eshelby, "The determination of the elastic field of an ellipsoidal inclusion, and related problems," Proc. R. Soc. London. Ser. A: Math. Phys. Sci. 241(1226), 376–396 (1957).
- ³²G. L. Gaines, Jr., *Insoluble Monolayers at Liquid-Gas Interfaces* (Wiley, New York, 1966).
- ³³A. W. Adamson, *Physical Chemistry of Surfaces* (Wiley, New York, 1990).
- ³⁴Y. Rotenberg, L. Boruvka, and A. W. Neumann, "Determination of surface tension and contact angle from the shapes of axisymmetric fluid interfaces," J. Colloid Interface Sci. 93, 169–183 (1983).
- ³⁵J. D. Berry, M. J. Neeson, R. R. Dagastine, D. Y. C. Chang, and R. F. Tabor, "Measurement of surface and interfacial tension using pendant drop tensiometry," J. Colloid Interface Sci. 454, 226–237 (2015).
- ³⁶S. Ji and M. Guvendiren, "Recent advances in bioink design for 3D bioprinting of tissues and organs," Front. Bioeng. Biotech. 5, 23 (2017).
- ³⁷R. Suntornnond, J. An, and C. K. Chua, "Bioprinting of thermoresponsive hydrogels for next generation tissue engineering: A review," Macromol. Mater. Eng. 302, 1600266 (2016).

https://doi.org/10.1121/10.0001068



- ³⁸U. Demirci and G. Montesano, "Single cell epitaxy by acoustic picolitre droplets," Lab Chip 7(9), 1139–1145 (2007).
- ³⁹E. H. Trinh, "Compact acoustic levitation device for studies in fluid dynamics and material science in the laboratory and microgravity," Rev. Sci. Instrum. 56(11), 2059–2065 (1985).
- ⁴⁰S. Fredericks and J. R. Saylor, "Experimental study of drop shape and wake effects on particle scavenging for non-evaporating drops using ultrasonic levitation," J. Aerosol Sci. 127, 1–17 (2019).
- ⁴¹P. L. Marston and E. H. Trinh, "Pseudo-extinction of light as a method for detecting acoustically induced shape oscillations of drops levitated in air," J. Acoust. Soc. Am. 77(S1), S20–S20 (1985).
- ⁴²M. Tokita and K. Hikichi, "Mechanical studies of sol-gel transition: Universal behavior of elastic modulus," Phys. Rev. A 35(10), 4329 (1987).
- ⁴³A. Chakrabarti, "Elastocapillary phenomena in soft elastic solids," Ph.D. thesis, Lehigh University, 2017.
- ⁴⁴Lord Rayleigh, *The Theory of Sound*, Reprinted 1945 ed. (Dover, London, 1894), Vol. 2.
- ⁴⁵M. S. Plesset and A. Prosperetti, "Bubble dynamics and cavitation," Ann. Rev. Fluid Mech. 9, 145–185 (1977).
- A. Prosperetti, "Free oscillations of drops and bubbles: The intial-value problem," J. Fluid Mech. 100, 333–347 (1980).
 A. Prosperetti, "Bubble dynamics—A review and some recent results,"
- ⁴⁷A. Prosperetti, "Bubble dynamics—A review and some recent results," Appl. Sci. Res. 38, 145–164 (1982).

- ⁴⁸L. A. Crum and A. Prosperetti, "Nonlinear oscillations of gas bubbles in liquids: An interpretation of some experimental results," J. Acoust. Soc. Am. 73, 121–127 (1983).
- ⁴⁹J. Bostwick and P. Steen, "Coupled oscillations of deformable spherical-cap droplets. Part 2. Viscous motions," J. Fluid Mech. 714, 336–360 (2013).
- ⁵⁰S. Davis, "Moving contact lines and rivulet instabilities. Part 1. The static rivulet," J. Fluid Mech. 98, 225–242 (1980).
- ⁵¹J. Bostwick and P. Steen, "Static rivulet instabilities: Varicose and sinuous modes," J. Fluid Mech. 837, 819–838 (2018).
- ⁵²J. Bostwick and P. Steen, "Stability of constrained capillary surfaces," Ann. Rev. Fluid Mech. 47, 539–568 (2015).
- ⁵³T. MacRobert, *Spherical Harmonics* (Pergamon, New York, 1967).
- ⁵⁴L. Rayleigh, "On the capillary phenomena of jets," Proc. R. Soc. London 29, 71–97 (1879).
- ⁵⁵A. C. Eringen, E. S. Suhubi, and C. C. Chao, "Elastodynamics, Vol. II, Linear theory," J. Appl. Mech. 45, 299 (1978).
- ⁵⁶R. C. Weast, *Handbook of Chemistry and Physics*, 52nd ed. (Chemical Rubber Company, Cleveland, OH, 1972).
- ⁵⁷E. Becker, W. J. Hiller, and T. A. Kowalewski, "Experimental and theoretical investigation of large-amplitude oscillations of liquid droplets," J. Fluid Mech. 231, 189–210 (1991).
- ⁵⁸R. W. Hyers, "Fluid flow effects in levitated droplets," Meas. Sci. Technol. 16, 394–401 (2005).